C. R. Palevol 16 (2017) 702–714

Contents lists available at ScienceDirect

Comptes Rendus Palevol

www.sciencedirect.com

Human Palaeontology and Prehistory

Is the deciduous/permanent molar enamel thickness ratio a taxon-specific indicator in extant and extinct hominids?

Le rapport d'épaisseur de l'émail des molaires déciduales/permanentes est-il un indicateur taxinomique chez les hominidés actuels et fossiles ?

Clément Zanolli[a,*], Priscilla Bayle[b], Luca Bondioli[c], M. Christopher Dean[d], Mona Le Luyer[b,e], Arnaud Mazurier[f], Wataru Morita[g], Roberto Macchiarelli[h,i]

[a] *UMR 5288 CNRS, Laboratoire AMIS, Université Toulouse-3 Paul-Sabatier, 31062 Toulouse, France*
[b] *UMR 5199 CNRS, Laboratoire PACEA, Université de Bordeaux, 33615 Bordeaux, France*
[c] *Sezione di Bioarcheologia, Museo Nazionale Preistorico Etnografico "Luigi Pigorini", Rome, Italy*
[d] *Department of Cell and Developmental Biology, University College London, London WC1E 6BT, UK*
[e] *School of Anthropology & Conservation, University of Kent, Canterbury, UK*
[f] *UMR 7285 CNRS, Institut de chimie des milieux et matériaux de Poitiers, Université de Poitiers, 86073 Poitiers, France*
[g] *Department of Oral Functional Anatomy, Graduate School of Dental Medicine, Hokkaido University, Hokkaido, Japan*
[h] *UMR 7194 CNRS, Laboratoire HNHP, Muséum national d'histoire naturelle, 75116 Paris, France*
[i] *Unité de formation Géosciences, Université de Poitiers, 86073 Poitiers, France*

ARTICLE INFO

Article history:
Received 7 April 2017
Accepted after revision 4 May 2017
Available online 16 June 2017

Handled by Roberto Macchiarelli and Clément Zanolii

Keywords:
Enamel
Dm2
M1
"Diphyodontic index"
Hominids

Mots clés :
Émail
Dm2
M1
« Indice diphyodonte »
Hominidés

ABSTRACT

In Primates, enamel thickness variation stems from an evolutionary interplay between functional/adaptive constraints (ecology) and the strict control mechanisms of the morphogenetic program. Most studies on primate enamel thickness have primarily considered the permanent teeth, while the extent of covariation in tooth enamel thickness distribution between deciduous and permanent counterparts remains poorly investigated. In this test study on nine extant and fossil hominids we investigated the degree of covariation in enamel proportions between 25 pairs of mandibular dm2 and M1 by a so-called "lateral enamel thickness diphyodontic index". The results did not provide an unambiguous picture, but rather suggest complex patterns likely resulting from the influence of many interactive factors. Future research should test the congruence of the "diphyodontic signal" between the anterior and the postcanine dentition, as well as between enamel and the enamel-dentine junction topography.

RÉSUMÉ

Chez les primates, le patron de variation d'épaisseur de l'émail est issu d'un compromis évolutif entre contraintes fonctionnelles/adaptatives (écologiques) et mécanismes de contrôle morphogénétique. La majorité des études portant sur l'épaisseur de l'émail des primates concerne les dents permanentes, tandis que le degré de covariation de distribution d'épaisseur de l'émail entre les équivalents déciduaux et permanents reste encore

* Corresponding author.
E-mail address: clement.zanolli@gmail.com (C. Zanolli).

http://dx.doi.org/10.1016/j.crpv.2017.05.002
1631-0683/

méconnu. Dans cette étude préliminaire, nous explorons le degré de covariation des proportions d'émail entre 25 paires de dm2 et M1 mandibulaires de neuf hominidés actuels et fossiles en élaborant un « indice diphyodonte d'épaisseur de l'émail latéral ». Les résultats ne montrent pas un signal évident, mais suggèrent plutôt des modèles complexes résultant probablement de l'influence d'interactions entre des facteurs variés. De futures recherches sur le sujet devraient tester le degré de congruence du « signal diphyodonte » entre les dents antérieures et post-canines, ainsi qu'entre l'émail et la topographie de la jonction émail–dentine.

1. Introduction

Following the pioneering methodological work developed by L.B. Martin for measurement procedure and standardization (Martin, 1985), the bi-three-dimensional assessment of tooth enamel thickness has become routine in taxonomic and adaptive/evolutionary studies of fossil and extant primates (e.g., Alba et al., 2013; Kono, 2004; Kono et al., 2014; Macchiarelli et al., 2004, 2009, 2013; Olejniczak et al., 2008a, 2008b, 2008c, 2008d; Pan et al., 2016; Skinner et al., 2015; Smith et al., 2003, 2005, 2011, 2012; Suwa et al., 2009; Zanolli et al., 2015, 2016a). Commonly used to infer durophagy and considered as a proxy of the dietary niches exploited by extinct species (e.g., Constantino et al., 2011, 2012; Lucas et al., 2008; Martin et al., 2003; Schwartz, 2000a; Teaford, 2007; Teaford and Ungar, 2015; Vogel et al., 2008), occlusal enamel thickness is seen as intimately related to dietary abrasiveness and selectively responsive to lifetime dental wear resistance (Pampush et al., 2013; Rabenold and Pearson, 2011).

In primates, enamel thickness variation stems from an evolutionary interplay between functional/adaptive constraints (ecology) and strict control mechanisms of the morphogenetic program (Horvath et al., 2014; Kelley and Swanson, 2008; Kono, 2004; Simmer et al., 2010; Smith et al., 2012; Vogel et al., 2008). It appears to respond relatively quickly in evolutionary time to dietary/ecological changes (Grine and Daegling, 2017; Hlusko et al., 2004; Le Luyer and Bayle, 2017), thus being prone to homoplasy (Smith et al., 2012; rev. in Macho, 2015).

Most studies on enamel thickness have primarily considered the permanent teeth, especially the molar series, while the extent of covariation in tooth enamel thickness between deciduous and permanent counterparts has been the object of limited quantitative analyses, including in hominids (for a recent synthesis and review of studies on deciduous enamel thickness in humans, see table 1 in Mahoney, 2013; additionally, among other contributions, see Benazzi et al., 2011; Fornai et al., 2014, 2016; Macchiarelli et al., 2006, 2013; Peretto et al., 2015; Zanolli, 2015a; Zanolli et al., 2010a, 2012, 2014). Accordingly, quantitative support to answer a number of questions remains so far elusive. More specifically: whenever, in a comparative intertaxonomic assessment, we score a permanent hominid tooth as relatively "thinly"- or "thickly-enamelled" and order it accordingly within a series of investigated specimens, does the primary element score similarly and does it (tend to) occupy a comparable position within the same deciduous series? Can we confidently predict an enamel thickness "category" for a hominid deciduous crown based on the measure of the permanent tooth (or vice versa)? Does a predictable deciduous-permanent pattern exist for tooth enamel thickness in hominids? If so, is it taxon-specific?

The second deciduous (dm2) and the first permanent (M1) molars are part of the same developmental molar series (rev. in Bailey et al., 2014, 2016; see also Evans et al., 2016), i.e., they are meristic elements with a similar and serially repeated structure within the same organism (Butler, 1956, 1967; Kraus and Jordan, 1965). In this study on some extant and fossil hominids, we thus investigate the degree of covariation in enamel proportions between the dm2 and the M1 (for the extant human condition, see Gantt et al., 2001; Grine, 2005; Huszár, 1972; Mahoney, 2010; Rossi et al., 1999). In order to perform intertaxonomic comparisons, we established a so-called "lateral enamel thickness diphyodontic index" (LETDI; see § Materials and methods) as a measure of the proportions in the amount of non-occlusal enamel (Macchiarelli et al., 2016; Zanolli, 2015b). Even if the mandibular dm2 and the M1 specifically used in this study are not successional elements, we introduced the wider concept of "diphyodontic index" referring to their usual differential use-life. Given the exploratory nature of this study, whose main goal is to capture a tendency or trend, if any, and not to assess intraspecific variation, or evolutionary trends, or phylogenetic relationships, the number of cases examined for each taxon (ranging from 1 to 5 tooth pairs) is just minimal. By definition, at this stage of the research the underlying assumption is that the signal revealed by each dm2-M1 crown pair used here, all from mandibular dentitions, represents the average condition of its own taxon, i.e., is taxon-representative.

Apart from some intertaxonomic differences in developmental timing and patterning between the dm2 and the M1 (Dean, 2000, 2006, 2010; Dean and Cole, 2013), given that the dm2 is in functional occlusion for a much shorter time and commonly experiences lower functional constraints at least until the weaning process begins (Fleagle, 2013; Swindler, 2002), we expect that, independently from their relative qualitative "category" ("thinner" vs. "thicker"), the dm2/M1 enamel relative volume ratios are < 1.

2. Materials and methods

The hominid taxa considered in this study include the four extant genera *Homo* (HOM), *Pan* (PAN), *Gorilla*

Table 1
List of the extant and fossil hominid taxa considered in the present study with their lateral enamel proportions of the second deciduous (dm2) and first permanent (M1) lower molars.
Tableau 1
Liste des taxons hominidés actuels et fossiles considérés dans la présente étude avec les proportions d'émail latéral des secondes molaires déciduales (dm2) et des premières molaires permanentes (M1) mandibulaires.

	Label	N crowns (specimens)	Collection/site	References
Extant taxa				
Homo	HOM	5 dm2s – 5 M1s	MNPELP; PBC	Original data
Pan	PAN	4 dm2s – 4 M1s	Univ. Poitiers & Univ. Toulouse, France	Original data
Gorilla	GOR	5 dm2s – 5 M1s	Univ. Poitiers & Univ. Toulouse, France	Original data
Pongo	PON	4 dm2s – 4 M1s	MZS; Univ. Toulouse, France	Original data
Fossil taxa				
Neanderthals	Nea	3 dm2s (RdM, S14–5, S42) 3 M1s (RdM, S14–7, S49)	Roc de Marsal (RdM) and Abri Suard (S), France	Bayle, 2008; Bayle et al., 2009; Macchiarelli et al., 2006; NESPOS Database, 2017
Paranthropus robustus	PAR	1 dm2 – 1 M1 (SK 63)	Swartkrans, South Africa	Original data
Australopithecus africanus	AUS	1 dm2 – 1 M1 (STS 24)	Sterkfontein, South Africa	Original data
Ouranopithecus macedoniensis	OUR	1 dm2 – 1 M1 (RPL–83)	Ravin de la Pluie, Macedonia, Greece	Macchiarelli et al., 2009
Oreopithecus bambolii	ORE	1 dm2 (FS1995#0009) 1 M1 (FS1996#Fi98)	Fiume Santo, Sardinia, Italy	Zanolli et al., 2010b, 2016a

MNPELP: Museo Nazionale Preistorico Etnografico "L. Pigorini", Rome, Italy; PBC: Pretoria Bone Collection, University of Pretoria, South Africa; MZS: Musée zoologique, Strasbourg, France.

(GOR) and *Pongo* (PON), and representatives of four fossil genera: the Plio-Pleistocene hominins *Paranthropus* (*robustus*) (PAR) and *Australopithecus* (*africanus*) (AUS), from the South African sites of Swartkrans and Sterkfontein, respectively, and the late Miocene European apes *Ouranopithecus* (*macedoniensis*) (OUR), from Macedonia, and *Oreopithecus* (*bambolii*) (ORE), from Sardinia. Besides *H. sapiens*, humans are also represented by the extinct Neanderthals (Nea). The existence of interspecific differences in molar enamel thickness has been ascertained within the australopith clade (e.g., Grine and Daegling, 2017; Grine and Martin, 1988; Olejniczak et al., 2008b; Pan et al., 2016; Skinner et al., 2015), but their consideration here is far beyond the specific purposes of our present work.

Details about the composition and origin of the mandibular dm2 and M1 specimens/samples are provided in Table 1. The extant human teeth, all from individuals of European origins, represent both sexes; conversely, no detailed information, including about their geographic provenance (and if from captive or wild individuals), is available to us regarding the extant great ape representatives. All pairs examined here are from single individuals, except for *Oreopithecus*. Because of the paucity of fossil materials suitable for such kind of analyses and the even more scanty number of currently available/accessible high-resolution records detailing the hominid tooth crown inner structure, in this first study we preferred to maximize the amount of signals, especially at generic level.

We have used the X-ray microtomographic record available to us of specimens which have been previously scanned at: the University of Poitiers, France, by a Viscom X8050-16 system (all extant taxa; original data); the ID 17 beam line of the European Synchrotron Radiation Facility of Grenoble, France (Neanderthals and *Oreopithecus*; Bayle, 2008; Bayle et al., 2009; Macchiarelli et al., 2006; NESPOS Database, 2017; Zanolli et al., 2010b, 2016a); the South African Nuclear Energy Corporation (Necsa), Pelindaba, by a Nikon XTH 225 ST equipment (*Paranthropus* and *Australopithecus*; original data); and the analytical platform set at the Bundesanstalt für Materialforschung und -prüfung (BAM) of Berlin, Germany (*Ouranopithecus*; Macchiarelli et al., 2008, 2009).

The data were reconstructed at a voxel size ranging from 21.0 to 83.2 μm, for the extant teeth, and from 21.6 to 50.0 μm, for the fossil specimens. Using Amira v.5.3 (Visualization Sciences Group Inc.) and ImageJ v.1.46 (Schneider et al., 2012), a semiautomatic threshold-based segmentation was carried out following the half-maximum height method (HMH; Spoor et al., 1993) and the region of interest thresholding protocol (ROI-Tb; Fajardo et al., 2002), taking repeated measurements on different slices of the virtual stack (Coleman and Colbert, 2007).

In order to avoid the problem of occlusal wear nearly invariably affecting at least the dm2 in most molar pairs, we uniquely considered lateral enamel. As lateral enamel thickness topography has a profound effect on crown morphology, it is expected to bring a taxon-specific signature, even if likely diluted compared to that provided by total enamel thickness that includes occlusal enamel (e.g., Kono and Suwa, 2008; Macchiarelli et al., 2013; Suwa et al., 2009). To quantify lateral enamel, the best-fit plane across the cervicoenamel line was firstly set on each crown and the tooth material below this basal plane eliminated (Olejniczak et al., 2008a). Then, a parallel plane to the former, tangent to the lowest enamel point of the occlusal basin, was defined and all material above it was also removed (Macchiarelli et al., 2013; Toussaint et al., 2010). Only the enamel and dentine portions between these two planes was preserved to estimate tissue proportions.

On the new set of virtually reduced and simplified crowns, five surface and volumetric variables were digitally measured (or calculated): LVe, the lateral volume of enamel (mm^3); LVcdp, the lateral volume of coronal dentine, including the lateral coronal aspect of the pulp chamber (mm^3); LSEDJ, the enamel-dentine junction (EDJ) lateral surface (mm^2); 3D LAET (= LVe/LSEDJ), the three-dimensional lateral average enamel thickness (mm); 3D LRET (= 100*3D LAET/(LVcdp$^{1/3}$)), the scale-free three-dimensional lateral relative enamel thickness. Intra- and interobserver tests for measurement accuracy run at different times by four observers revealed differences < 4%. For the taxa with N > 1, we have firstly computed the LETDI for each dm2/M1 pair and then calculated the average value.

Pearson correlation tests among the variables listed above show that, in each molar pair, the 3D lateral relative enamel thickness (3D LRET) exhibits the highest correlation ($p < 0.01$ vs. $p < 0.02$ for 3D LAET and $p < 0.05$ for LVE). A "lateral enamel thickness diphyodontic index" (LETDI) has been thus calculated as follows: 3D $LRET_{dm2}$/3D $LRET_{M1}$. Statistical analyses were performed with R v.3.2.1 (R Development Core Team, 2017).

To visualize similarities vs. differences in enamel thickness topography within an assemblage of such variably sized and shaped teeth, *ad hoc* imaging techniques were used to virtually unroll lateral enamel and to project it into standardized morphometric maps (Bayle et al., 2011; Bondioli et al., 2010; Macchiarelli et al., 2013; for similar imaging techniques, see also Dowdeswell et al., 2017; Morita et al., 2016, 2017; Puymerail, 2011; Puymerail et al., 2012a, 2012b; Tsegai et al., 2017). Because each morphometric map (MM) is scaled according to the maximal value of the analysed tooth, the patterns expressed by the dm2s and the M1s are independent from the absolute and relative enamel thickness values. By using a custom routine developed in R v.3.2.1 (R Development Core Team, 2017) with the packages spatstat (Baddeley et al., 2015) and gstat (Pebesma, 2004), enamel thickness values were standardized between 0 and 1 and each morphometric map was set within a grid of 40 columns and 180 rows. We then performed a between-group principal component analysis (bgPCA; Mitteroecker and Bookstein, 2011) based on the standardized morphometric map outputs with the package Morpho v.2.4.1.1 (Schlager, 2017) for R v.3.3.3 (R Development Core Team, 2017).

3. Results

The scatterplot of the lateral relative enamel thickness of the dm2 (3D $LRET_{dm2}$) against the M1 values (3D $LRET_{M1}$) of all individual and composite (*Oreopithecus*) tooth pairs used in this study is shown in Fig. 1. We observe little variation among the four extant hominid genera, *Gorilla* and *Pan* tending to align with the regression line, whereas *Pongo* and humans scatter slightly more on both side of this line. Globally, the fossil taxa do not deviate much more than the extant hominids, *Australopithecus* and *Paranthropus* being as distant from the regression line as the farthest extant human are. In this context, the composite individual representing *Oreopithecus* behaves like *Pan*.

For the ten hominid taxa, the 3D LRET values and those of the LETDI "diphyodontic index" are shown in Table 2. For the $LRET_{dm2}$, *Ouranopithecus* (12.0), *Paranthropus* and the *Australopithecus* from Sterkfontein (both 10.9) show absolutely thick enamel, while *Pongo* and *Gorilla* (global range: 4.7–6.3) and *Oreopithecus* (6.0) are relatively thin-enamelled. A difference was noticeable between the two African apes, *Pan* having thicker enamel (6.3–8.9), but on average still thinner than measured in extant humans (8.0–9.2). Enamel in Neanderthals is thinner compared to the extant values (6.4–7.1). As a whole, the decreasing order for the lateral relative enamel thickness of the lower dm2 is as follows: *Ouranopithecus* > *Paranthropus* = *Australopithecus* > extant humans ≥ *Pan* ≈ Neanderthals > *Oreopithecus* > *Gorilla* ≈ *Pongo*, the variation interval covered by 3D LRET being comprised between 12.0 and 4.7.

Three sets are identifiable for the 3D $LRET_{M1}$: the first distinguishes the absolutely thickly-enamelled *Paranthropus* (15.6) and *Ouranopithecus* (13.4), the second assembles the variably intermediate *Homo* (all taxa), *Pan*, *Australopithecus* and *Oreopithecus* (range: 8.3–11.8), while the third includes the thinly-enamelled *Gorilla* and *Pongo* (range: 5.9–8.1). In this context, *Pan* (8.8–11.8) is indistinguishable from the extant human condition (9.3–11.2). The Neanderthal range (8.3–9.1) fits the value obtained for *Oreopithecus* (9.2). Here, the decreasing pattern is as follows: *Paranthropus* > *Ouranopithecus* > *Australopithecus* ≥ extant humans ≈ *Pan* ≥ *Oreopithecus* ≈ Neanderthals > *Gorilla* ≈ *Pongo*, the values globally ranging from 15.6 to 5.9.

The last column of Table 2 presents the values of the LETDI ratio. LETDI ranges in the whole sample from 0.63 in a *Pongo* individual and 0.65 in *Oreopithecus*, to 0.98 in *Australopithecus* and 0.99 in an extant human (Fig. 2). The totality of the ratios are < 1.0. According to this parameter, even if distinct for its greater amount of enamel, *Paranthropus* (0.70) is closer to *Oreopithecus* (0.65) than to *Ouranopithecus* (0.89), with which it otherwise shares thickly-enamelled dm2 and M1. Within our limited set of investigated cases, *Pongo* and extant humans display larger variation than Neanderthals and the African apes (Fig. 2).

Distinctly for each taxon and for each molar type, the standardized morphometric maps (MM) imaging the virtually unrolled and projected lateral enamel are shown in Fig. 3. For the extant taxa and Neanderthals, they represent consensus maps generated by merging the available individual records into a single dataset and subsequently calculating the interpolation (Puymerail, 2011; Puymerail et al., 2012a, 2012b). Because each MM is scaled according to the maximal value of the analysed tooth, the patterns expressed by the dm2s and the M1s are independent from the absolute and relative enamel thickness values.

In all taxa and both molars, enamel decreases cervically. For the dm2, thickening is commonly found buccally; however, thickening in *Ouranopithecus* is more evenly distributed around most of the subocclusal contour. The extant human pattern is close to that displayed by the Neanderthal deciduous molars. The African apes and, to a lesser extent, *Pongo* as well, share similar enamel distribution. In this context, the least contrasted map is that of *Paranthropus*, which is distinct from *Australopithecus* and, mostly, from *Ouranopithecus*, but which in turn recalls that

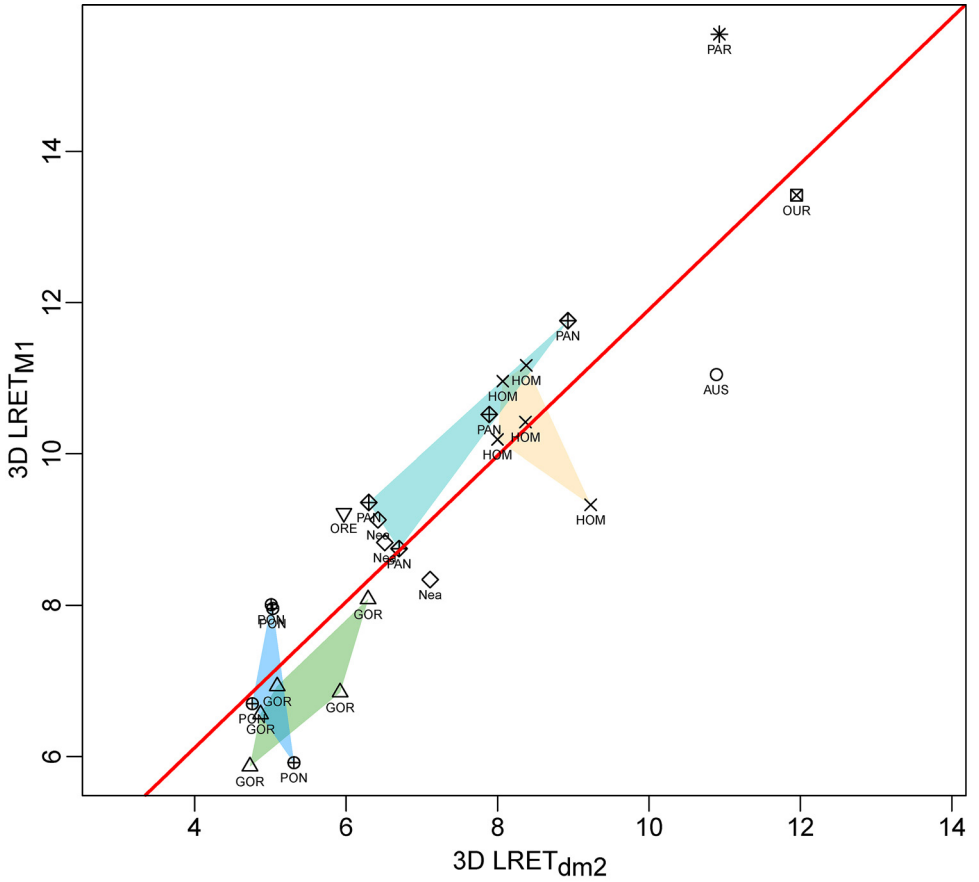

Fig. 1. Scatterplot of the 3D lateral relative enamel thickness values of the dm2 (3D LRET$_{dm2}$) against the M1 (3D LRET$_{M1}$) comparatively assessed in four extant (HOM, PAN, GOR, PON) and five fossil hominid taxa (Nea, PAR, AUS, OUR, ORE). The red line represents the regression line of the 3D LRET$_{dm2}$ against 3D LRET$_{M1}$. AUS: *Australopithecus* (*africanus*); GOR: *Gorilla* (sp.); HOM: extant humans; Nea: Neanderthals; ORE: *Oreopithecus* (*bambolii*); OUR: *Ouranopithecus* (*macedoniensis*); PAN: *Pan* (sp.); PAR: *Paranthropus* (*robustus*); PON: *Pongo* (sp.).

Fig. 1. Graphique représentant l'indice tridimensionnel d'épaisseur relative de l'émail latéral des dm2s (3D LRET$_{dm2}$) en fonction des M1s (3D LRET$_{M1}$) pour quatre genres hominidés actuels (HOM, PAN, GOR, PON) et cinq taxons fossiles (Nea, PAR, AUS, OUR, ORE). La ligne rouge représente la droite de régression de 3D LRET$_{dm2}$ en fonction de 3D LRET$_{M1}$. AUS : *Australopithecus* (*africanus*) ; GOR : *Gorilla* (sp.) ; HOM : humains actuels ; Nea : Néandertaliens ; ORE : *Oreopithecus* (*bambolii*) ; OUR : *Ouranopithecus* (*macedoniensis*) ; PAN : *Pan* (sp.) ; PAR : *Paranthropus* (*robustus*) ; PON : *Pongo* (sp.).

of *Oreopithecus*. In the MMs of the M1s, thickening is not mainly concentrated buccally, as seen for the dm2s, but more commonly spread buccally/mesiobuccally and also lingually/distolingually. However, this is not exactly the case in *Ouranopithecus* and, to a lesser extent, in *Oreopithecus*, where thickening is essentially concentrated mesiolingually, in the former, and distolingually, in the latter. All extant and extinct human representatives show a similar pattern resembling that of *Australopithecus*. Here again, the signatures displayed by the African apes are similar to the pattern revealed by *Pongo*, which in turn recalls that of *Paranthropus*. Finally, in terms of intertooth polarity of the signal, the most similar MMs are those of the extant apes (notably *Gorilla* and *Pongo*), while distinct topographic differences are appreciable in *Paranthropus* and *Oreopithecus*.

The bgPCA based on the MM scores only provides modest discrimination among the taxa along both bgPC axes (PC1: 56.37%, PC2: 31.11%). However, the representatives of all extant and fossil hominins (HOM, Nea, PAR, AUS) tend to regroup on the positive aspect of bgPC1, whereas the extant apes (PAN, GOR and PON) mostly fall in the negative values along this axis (Fig. 4). The two Miocene hominids (OUR and ORE) show distinct signals, *Ouranopithecus* being intermediate between *Pongo* and *Homo*, while *Oreopithecus* more closely resembles *Gorilla*. The specimens in the positive space of bgPC1 display evenly spread relatively thicker enamel deposited towards the more occlusal portion of the entire surface, while the specimens in the negative space of bgPC1 have two vertically projected thickened "pillars" on the buccal and lingual aspects, respectively, separated by two large strips of thinner enamel nearly covering the entire mesial and distal crown sides. Along bgPC2, taxonomic discriminations are weak (Fig. 4).

The correlation between LETDI and body mass is shown in Fig. 5. Varying from good (notably in extant humans, but also in Neanderthals, *Pan* and *Ouranopithecus*) to modest (in *Gorilla*, *Pongo* and *Paranthropus*), a certain linear agreement is detectable in both smaller- and larger body-sized taxa. However, even ignoring the perhaps biased signal from the *Oreopithecus* composite representative, also

Table 2
Three-dimensional lateral relative enamel thickness (3D LRET) of the second deciduous (dm2) and the first permanent (M1) lower molars and "lateral enamel thickness diphyodontic index" (LETDI: 3D $LRET_{dm2}$/3D $LRET_{M1}$) comparatively assessed in four extant (HOM, PAN, GOR, PON) and five fossil hominid taxa (Nea, PAR, AUS, OUR, ORE). In parentheses, the number of examined molar pairs.
Tableau 2
Indice tridimensionnel d'épaisseur relative de l'émail latéral (3D LRET) des deuxièmes molaires déciduales (dm2) et des premières molaires permanentes (M1) inférieures et « indice diphyodonte d'épaisseur de l'émail latéral » (LETDI : 3D $LRET_{dm2}$/3D $LRET_{M1}$) comparés chez quatre genres hominidés actuels (HOM, PAN, GOR, PON) et cinq taxons fossiles (Nea, PAR, AUS, OUR, ORE). Le nombre de paires de molaires examinées est indiqué entre parenthèses.

Taxon		3D $LRET_{dm2}$	3D $LRET_{M1}$	LETDI
HOM	Mean	8.4	10.4	0.81
	Range (5)	*8.0–9.2*	*9.3–11.2*	*0.74–0.99*
Nea	Mean	6.7	8.8	0.76
	Range (3)	*6.4–7.1*	*8.3–9.1*	*0.70–0.85*
PAN	Mean	7.5	10.1	0.74
	Range (4)	*6.3–8.9*	*8.8–11.8*	*0.67–0.77*
GOR	Mean	5.4	6.9	0.79
	Range (5)	*4.7–6.3*	*5.9–8.1*	*0.73–0.86*
PON	Mean	5.0	7.2	0.72
	Range (4)	*4.8–5.3*	*5.9–8.0*	*0.63–0.90*
PAR		10.9	15.6	0.70
AUS		10.9	11.1	0.98
OUR		12.0	13.4	0.89
ORE		6.0	9.2	0.65

AUS: *Australopithecus* (*africanus*); GOR: *Gorilla* (sp.); HOM: extant humans; Nea: Neanderthals; ORE: *Oreopithecus* (*bambolii*); OUR: *Ouranopithecus* (*macedoniensis*); PAN: *Pan* (sp.); PAR: *Paranthropus* (*robustus*); PON: *Pongo* (sp.).

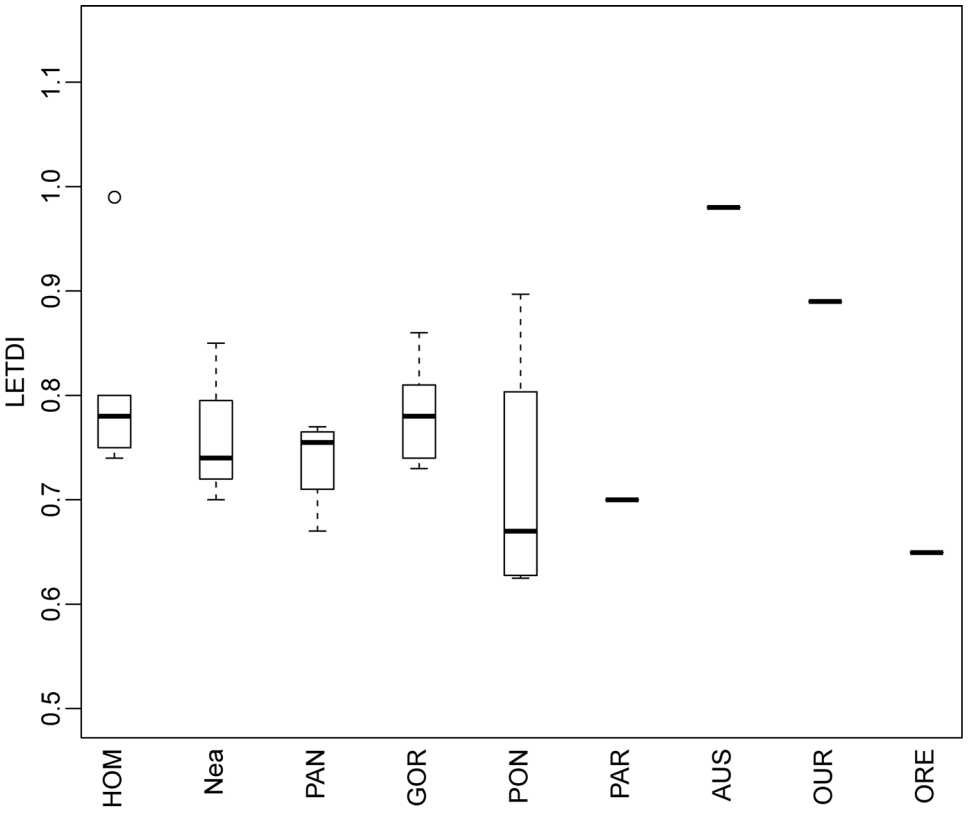

Fig. 2. Boxplots of the "lateral enamel thickness diphyodontic index" (LETDI) comparatively assessed in four extant (HOM, PAN, GOR, PON) and five fossil hominid taxa (Nea, PAR, AUS, OUR, ORE). AUS: *Australopithecus* (*africanus*); GOR: *Gorilla* (sp.); HOM: extant humans; Nea: Neanderthals; ORE: *Oreopithecus* (*bambolii*); OUR: *Ouranopithecus* (*macedoniensis*); PAN: *Pan* (sp.); PAR: *Paranthropus* (*robustus*); PON: *Pongo* (sp.). The boxplot shows the median, the range (lower and upper whisker), the first quartile (lower hinge) and the last quartile (upper hinge).
Fig. 2. Graphique illustrant le degré de variation de « l'indice diphyodonte d'épaisseur de l'émail latéral » (LETDI) estimé chez quatre genres d'hominidés actuels (HOM, PAN, GOR, PON) et cinq taxons fossiles (Nea, PAR, AUS, OUR, ORE). AUS : *Australopithecus* (*africanus*) ; GOR : *Gorilla* (sp.) ; HOM : humains actuels ; Nea : Néandertaliens ; ORE : *Oreopithecus* (*bambolii*) ; OUR : *Ouranopithecus* (*macedoniensis*) ; PAN : *Pan* (sp.) ; PAR : *Paranthropus* (*robustus*) ; PON : *Pongo* (sp.). Les boîtes à moustaches montrent la médiane, les limites de variation (moustaches inférieure et supérieure), le premier quartile (partie inférieure de la boite) et le dernier quartile (partie supérieure de la boîte).

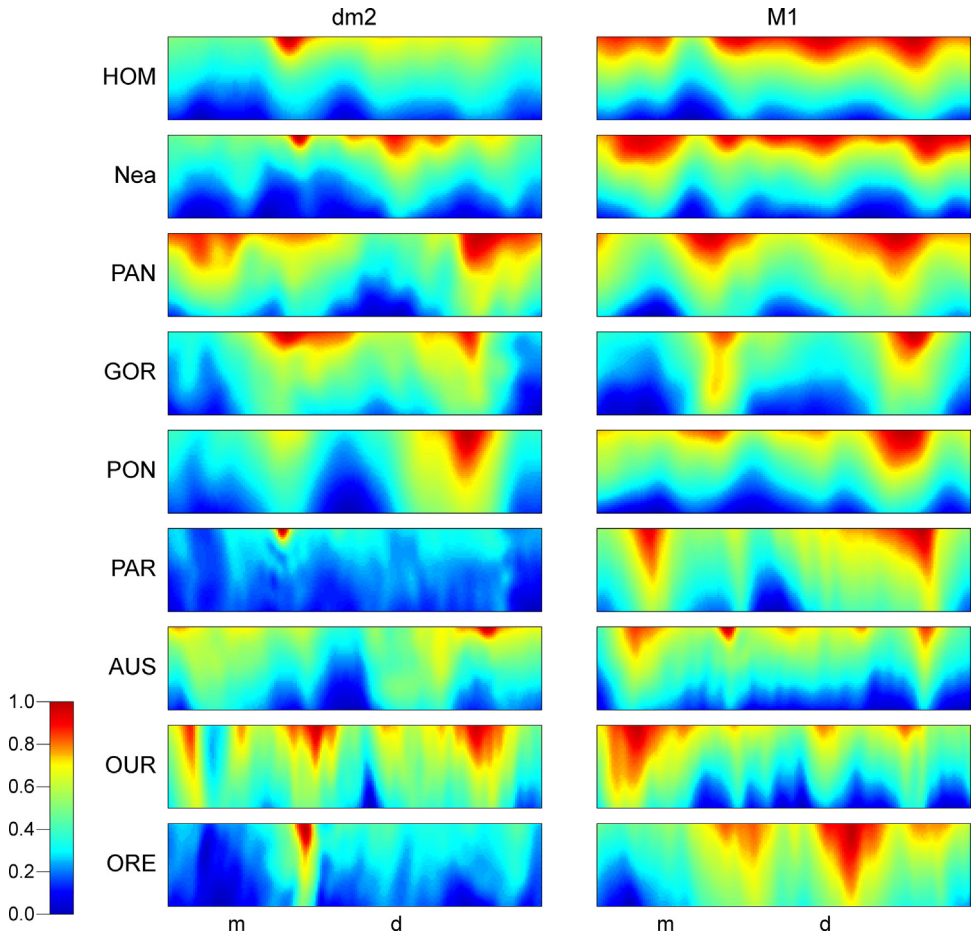

Fig. 3. Standardized morphometric maps of the lateral enamel thickness of the dm2 (left column) and M1 (right) in four extant (HOM, PAN, GOR, PON) and five fossil hominid taxa (Nea, PAR, AUS, OUR, ORE) rendered by a chromatic scale ranging from thin (blue) to thick (red). For the extant taxa and Neanderthals, the consensus maps representing the "average" condition are shown. AUS: *Australopithecus* (*africanus*); GOR: *Gorilla* (sp.); HOM: extant humans; Nea: Neanderthals; ORE: *Oreopithecus* (*bambolii*); OUR: *Ouranopithecus* (*macedoniensis*); PAN: *Pan* (sp.); PAR: *Paranthropus* (*robustus*); PON: *Pongo* (sp.); m: mesial; d: distal.

Fig. 3. Cartographies morphométriques standardisées de l'épaisseur de l'émail latéral des dm2 (colonne de gauche) et des M1 (colonne de droite) chez quatre genres d'hominidés actuels (HOM, PAN, GOR, PON) et cinq taxons fossiles (Nea, PAR, AUS, OUR, ORE) représentées par une échelle chromatique allant d'un émail fin (bleu) à épais (rouge). Pour les taxons actuels et les Néandertaliens, les cartes consensus représentant la condition « moyenne » sont illustrées. AUS : *Australopithecus* (*africanus*) ; GOR : *Gorilla* (sp.) ; HOM : humains actuels ; Nea : Néandertaliens ; ORE : *Oreopithecus* (*bambolii*) ; OUR : *Ouranopithecus* (*macedoniensis*) ; PAN : *Pan* (sp.) ; PAR : *Paranthropus* (*robustus*) ; PON : *Pongo* (sp.) ; m : mésial ; d : distal.

Australopithecus behaves here as an outlier, a result which deserves confirmation from the inclusion in the analysis of the signal from additional individuals. Interestingly, extant humans and *Gorilla*, which display comparable average LETDIs, differ in average body mass and the two largest-sized taxa considered in our analysis, *Gorilla* and *Ouranopithecus*, provided distinct LETDI ratios.

4. Discussion

A limiting/complicating factor in our analytical approach is the use of non-occlusal enamel compared to the information imprinted occlusally, or even at specific cuspal level (e.g., Grine, 2005; Kono et al., 2002; Macho and Berner, 1993; Mahoney, 2010; Schwartz, 2000b). However, lateral enamel has its own signals that have never been previously explored as a functional unit independent of occlusal enamel thickness. In this sense, our study attempts to do this for the first time. While occlusal enamel topography is more directly informative in terms of functional activity and adaptive responses (e.g., Guy et al., 2013; Kono, 2004; Kono and Suwa, 2008; Olejniczak et al., 2008b), lateral enamel thickness is also involved in dissipating occlusally-related stresses (Benazzi et al., 2013a, 2013b). Lateral enamel also resists wear, tooth height loss and maintains interproximal tooth-tooth contacts during the late stages of tooth wear after dentine exposure over the occlusal surface. Final loss of lateral enamel marks the breakdown of the dentition (Dean et al., 1992) and is significant in the life history of individuals. Nonetheless, it is also possible that the use of the entirely unrolled lateral crown band introduced inessential, or even somehow noisy information. In fact, while individual morphometric maps clearly reveal site-specific differences

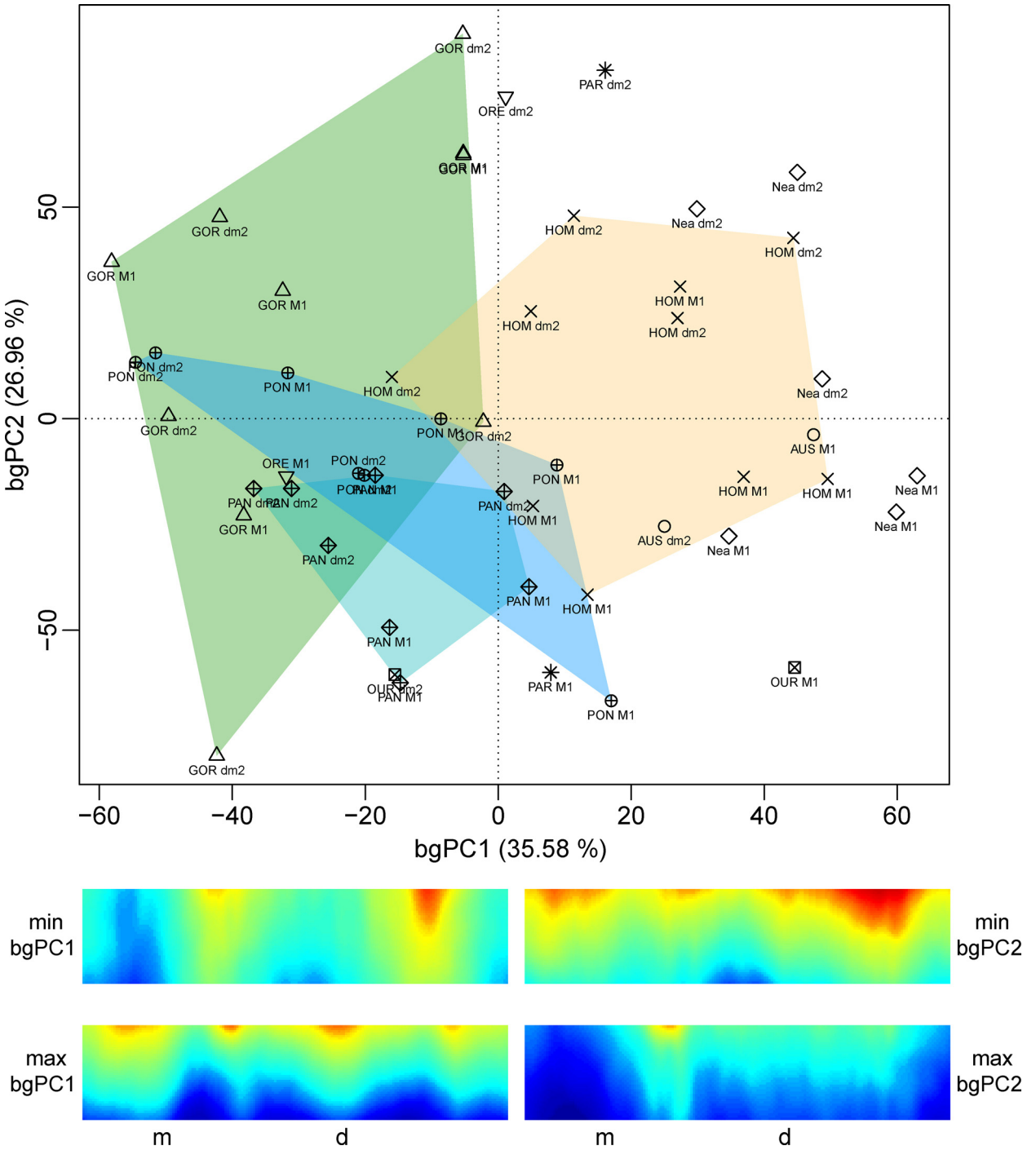

Fig. 4. bgPCA plot based on the standardized morphometric maps (MM) of the dm2 and M1 of four extant (HOM, PAN, GOR, PON) and five fossil hominid taxa (Nea, PAR, AUS, OUR, ORE). The MMs below the plot show the extreme conditions along bgPC1 and bgPC2. AUS: *Australopithecus* (*africanus*); GOR: *Gorilla* (sp.); HOM: extant humans; Nea: Neanderthals; ORE: *Oreopithecus* (*bambolii*); OUR: *Ouranopithecus* (*macedoniensis*); PAN: *Pan* (sp.); PAR: *Paranthropus* (*robustus*); PON: *Pongo* (sp.); m: mesial; d: distal.

Fig. 4. Graphique bgPCA basé sur les cartes morphométriques standardisées (MM) des dm2 et M1 chez quatre genres d'hominidés actuels (HOM, PAN, GOR, PON) et cinq taxons fossiles (Nea, PAR, AUS, OUR, ORE). Les MM sous le graphique montrent les conformations extrêmes le long de bgPC1 et bgPC2. AUS : *Australopithecus* (*africanus*) ; GOR : *Gorilla* (sp.) ; HOM : humains actuels ; Nea : Néandertaliens ; ORE : *Oreopithecus* (*bambolii*) ; OUR : *Ouranopithecus* (*macedoniensis*) ; PAN : *Pan* (sp.) ; PAR : *Paranthropus* (*robustus*) ; PON : *Pongo* (sp.) ; m : mésial ; d : distal.

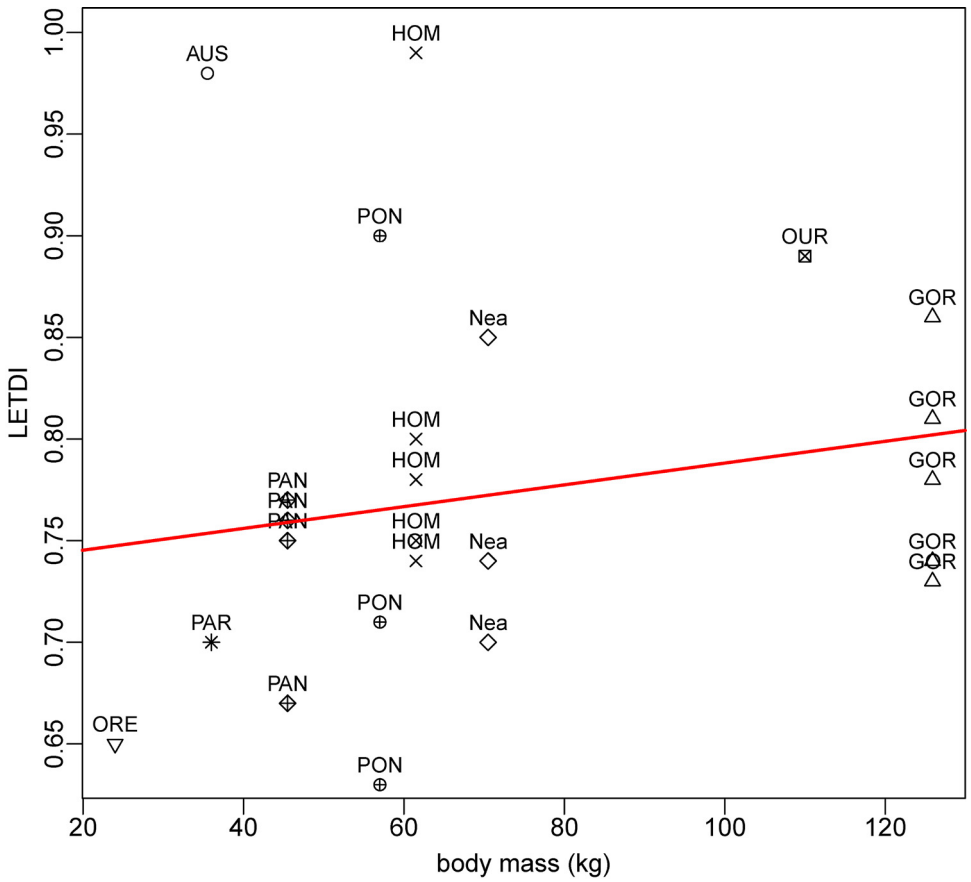

Fig. 5. Values of the "lateral enamel thickness diphyodontic index" (LETDI) compared with body mass estimates (average values, from Fleagle, 2013) in four extant (HOM, PAN, GOR, PON) and five fossil hominid taxa (Nea, PAR, AUS, OUR, ORE). The red line represents the regression line of the body mass against the LETDI. AUS: *Australopithecus* (*africanus*); GOR: *Gorilla* (sp.); HOM: extant humans; Nea: Neanderthals; ORE: *Oreopithecus* (*bambolii*); OUR: *Ouranopithecus* (*macedoniensis*); PAN: *Pan* (sp.); PAR: *Paranthropus* (*robustus*); PON: *Pongo* (sp.).

Fig. 5. Valeurs de « l'indice diphyodonte d'épaisseur de l'émail latéral » (LETDI) comparées aux estimations de masse corporelle (valeurs moyennes, d'après Fleagle, 2013) pour quatre genres d'hominidés actuels (HOM, PAN, GOR, PON) et cinq taxons fossiles (Nea, PAR, AUS, OUR, ORE). La ligne rouge représente la droite de régression de la taille corporelle en fonctions de l'indice LETDI. AUS : *Australopithecus* (*africanus*) ; GOR : *Gorilla* (sp.) ; HOM : humains actuels ; Nea : Néandertaliens ; ORE : *Oreopithecus* (*bambolii*) ; OUR : *Ouranopithecus* (*macedoniensis*) ; PAN : *Pan* (sp.) ; PAR : *Paranthropus* (*robustus*) ; PON : *Pongo* (sp.).

among the compartments which relate to occlusal cusp shape and topography (Fig. 3), at this stage we did not yet decompose the band into its mesial, distal, buccal and lingual components, and did not examine and compare their sometimes distinctly heterogeneous signatures. This task we would expect to limit the effects of differences in tooth crown architecture, notably outer surface convexity and intercuspal groove depth and extension. This, will in any case require additional research and the development of *ad hoc* analytical protocols, also because the outline shape of the dm2s and M1s used in this study tends to differ and, notably in the case of intertaxonomic analyses using variably-shaped tooth crowns, a risk of comparing not exactly homologous spots exists.

The expectation, formulated in a purely functional perspective, of LETDI ratios < 1.0 (the M1 crown being in principle equipped with a thicker coating of enamel for resisting higher and prolonged wear-inducing loads) is not fully satisfied by the present results (for enamel proportions in extant human lower dm1s-dm2s-M1s, see Mahoney, 2010). In two representatives from as many taxa it is close to be falsified: an extant human individual (0.99), and the *Australopithecus* representative (0.98), even if the large majority of the ratios are around or below 0.8. The two minima for the LETDI correspond to *Oreopithecus* (0.65, a value obtained from two individuals, thus prone to bias) and *Paranthropus* (0.70). This is interesting, and may be relevant whenever confirmed by additional data, as it might indicate that a large difference between the dm2 and the M1 in the proportional amount of enamel volume deposited along the crown walls occurs in both absolutely thickly-enamelled and relatively thinly-enamelled hominids. In any case, the results (Table 2, Fig. 2) show also that the opposite can occur, i.e., that the deciduous and permanent molars of both thickly-enamelled hominids (e.g., *Ouranopithecus*) and representatives of relatively thinly-enamelled taxa (e.g., *Gorilla*, *Pongo*) may present comparable values of lateral relative enamel thickness (3D LRET). In sum, even if present results tend to support the evidence that primate "deciduous teeth have thinner enamel than permanent

teeth" (Swindler, 2002: 14), including in humans (Mahoney, 2010), the extent of their enamel proportions, at least for non-occlusal enamel, appears rather variable.

By definition, the study assumed that the signal revealed by each dm2-M1 crown pair represents the average condition of their own taxon (including for the composite *Oreopithecus* representative). However, even if molar enamel thickness does not seem to behave as sexually dimorphic (e.g., Hlusko, 2016; Hlusko et al., 2004; Rossi et al., 1999), a growing body of evidence indicates a considerable amount of interspecific temporal and geographic variation (e.g., Kato et al., 2014; Smith et al., 2011, 2012). Conversely, the extent of intraspecific variation ranges in most cases from poorly reported to simply unknown, and even in extant humans enamel thickness chrono-geographic variation is far from being appropriately documented (Le Luyer and Bayle, 2017) and, with very few exceptions (e.g., Feeney et al., 2010; Grine, 2005), most currently available information is limited to European or European-derived population samples (rev. in Le Luyer, 2016; see Zanolli et al., 2017). At any rate, the present evidence based on the limited number of African apes represented here suggests variation in lateral enamel thickness may be similarly large in both deciduous and permanent molars (Table 2).

To interpret the "lateral enamel thickness diphyodontic index" more comprehensively – or indeed any other kind of "enamel thickness diphyodontic index" (ETDI) suitable for appropriately assessing the deciduous-permanent tooth enamel volume proportions (and its distribution pattern as well) – a number of biological, behavioural and ecological factors should be taken into account.

The four extant and four extinct hominid genera represented in our analysis are known for exploiting, or are reported to have exploited, respectively, a wide range of food resources in a variety of diverse environments (Fleagle, 2013; Guatelli-Steinberg, 2016; Hartwig, 2002; Merceron et al., 2005; Nelson and Rook, 2016; Scott et al., 2005; Sponheimer and Lee-Thorp, 2015; Ungar, 2007; Ungar and Sponheimer, 2013). Depending on the taxon-specific feeding habits, the time spent feeding may be considered as another variable which, together with food abrasiveness, likely plays a role in the selection of enamel thickness because of dental wear resistance, i.e., adaptation is not only resistance to fracture, but also to prolonged periods of wear to which enamel thickness can be related (Grine and Daegling, 2017; Pampush et al., 2013). The investigative tool used here – the LETDI – did not reveal any immediately obvious link with known dietary and/or ecological niche; for example, relative medium-low (< 0.80) values are shared by Neanderthals, *Pan*, *Gorilla*, *Pongo*, *Paranthropus* and *Oreopithecus*, while extant humans, *Australopithecus* and *Ouranopithecus* provided medium-high values (> 0.80). We note, anyhow, that in the bgPCA of the morphometric maps (Fig. 4): the more folivorous taxa (*Pan*, *Gorilla*, and perhaps *Oreopithecus*) tend to be in the negative space of bgPC1; *Pongo*, a slightly more diversified folivorous/frugivorous feeder, is found in the positive space of bgPC1; the omnivorous humans are mostly scattered across the positive space of bgPC1 and the positive space of bgPC2; *Paranthropus* and *Australopithecus*, which likely also with *Ouranopithecus* relied on diverse diets but shared the inclusion of hard/gritty food items, are found in the positive part of bgPC1, but scattered along bgPC2 (Fig. 4); finally, *Ouranopithecus* sets in the negative space of bgPC2, the dm2 and M1 being spread along the bgPC1 axis. In sum, even if we agree the reliability of enamel thickness as a dietary indicator breaks down in some cases where phylogenetically closely-related species that consume different amounts of hard items are considered (Grine and Daegling, 2017), at a first glance, differences in "dental ecology" (*sensu* Cuozzo et al., 2012) seem to play a role in affecting the polarity of the dm2/M1 ratio used in the present study. If so, additional research – using any kind of *ad hoc* ETDI – should be performed on the anterior teeth.

The taxa investigated here are also diverse in body mass (Fleagle, 2013; Hemmer, 2015), a variable that in extant primates is correlated to a number of life history attributes (e.g., weaning age, age at maturity, age at first breeding in females), as well as to tooth size (e.g., molar crown area) (rev. in Hemmer, 2015). Even if our current analyses comparing LETDI with body size only shows limited linear correlation between these variables, it still represents a promising research track for the future.

Our "diphyodontic index" seems to be poorly or not related to the age at eruption of the first lower permanent molar, another key life history trait which in hominins marks the end of infancy (Kelley and Bolter, 2013). In fact, while also a strong genetic contribution to variation in timing of primary tooth emergence is well documented in humans (Chan et al., 2012), and likely also in hominids (Swindler, 2002), the LETDIs of *Pan* and of the *Australopithecus* representative used here that, for example, show comparable ages at LM1 eruption (Hemmer, 2015: table 15), differ markedly.

5. Concluding remarks

In a previous study, we noted that "some evidence suggests deciduous versus permanent molar enamel thickness distribution and relative proportions vary among extant and fossil hominid taxa... Inner signatures extracted from the primary and secondary dentition, respectively, may or may not provide similar/comparable pictures of time-related intrataxic evolutionary changes in tooth tissue proportions" (Macchiarelli et al., 2013: 259). The results collected from the present exploratory test using a newly developed analytical tool – the "lateral enamel thickness diphyodontic index" (LETDI) – did not, however, provide an unambiguous and immediately readable picture, as might otherwise have been predictable on the basis of some ontogenetic and morphological studies using sequential teeth (e.g., Bailey et al., 2014, 2016; Evans et al., 2016). Rather, our results suggest complex patterns that likely result from the influence of a number of interactive factors. Increasing evidence exists for lifetime-related enamel thickness and dietary wear association in extant primates (e.g., Pampush et al., 2013) and positive selection for adaptation in human evolution has been shown for the genes coding for the enamel matrix proteins (e.g., Daubert et al., 2016; Horvath et al., 2014). However, given also the high phenotypic plasticity of enamel thickness (e.g., Hlusko,

2016; Kato et al., 2014; Smith et al., 2012), it is possible that a fraction of the signal provided by any kind of tooth enamel "diphyodontic index" is non-adaptive, or that the degree of adaptability and functional significance of this trait varies topographically across the dentition. With this respect, together with some methodological advancement in the identification of the most reliable parameters and tooth crown areas to be considered for intertaxonomic investigations, a fruitful area of research would be to test the congruence of the "diphyodontic signal" between the anterior and the postcanine dentition, as well as between enamel and the enamel-dentine junction topography.

Acknowledgements

The present study contributes to the Palevol thematic issue "Hominin biomechanics, virtual anatomy and inner structural morphology: From head to toe. A tribute to Laurent Puymerail", promoted by C.Z. and R.M. Our friend and colleague Laurent was among the developers of the "unrolling" routine used in this study, and also provided relevant conceptual inputs. With his innovative and thoughtful work, only developed along a terribly short time, Laurent marked the field of "virtual palaeoanthropology". We acknowledge also his elegant style and sharp intellect. We really miss him.

For having granted or facilitated the access to the materials used in this study, we are very grateful to J.-J. Cleyet-Merle (Les Eyzies-de-Tayac), L. de Bonis (Poitiers), D. Grimaud-Hervé (Paris), G. Koufos (Thessaloniki), S. Potze (Pretoria), L. Rook (Florence), F. Sémah (Paris), F. Thackeray (Johannesburg), J.-F. Tournepiche (Angoulême), L. Trebini (Sassari), H. Widianto (Jakarta), M.D. Wandhammer (Strasbourg). The microtomographic records of the specimens detailed outside the platform set at the Univ. of Poitiers have been realized thanks to the support provided by A. Bravin (Grenoble), F. de Beer (Pelindaba-Johannesburg), J. Hoffman (Pelindaba-Johannesburg), B. Illerhaus (Berlin), C. Nemoz (Grenoble), P. Tafforeau (Grenoble). For discussion, we acknowledge D.M. Alba (Barcelona), J. Braga (Toulouse), F.E. Grine (Stony Brook), J. Kelley (Tempe), L. Rook (Florence).

References

Alba, D.M., Fortuny, J., Pérez de los Ríos, M., Zanolli, C., Almécija, S., Casanovas-Vilar, I., Robles, J.M., Moyà-Solà, S., 2013. New dental remains of *Anoiapithecus* and the first appearance datum of hominoids in the Iberian Peninsula. J. Hum. Evol. 65, 573–584.

Baddeley, A., Rubak, E., Turner, R., 2015. Spatial Point Patterns: Methodology and Applications. R. Chapman and Hall/CRC Press, London.

Bailey, S.E., Benazzi, S., Buti, L., Hublin, J.-J., 2016. Allometry, merism and tooth shape of the lower second deciduous molar and first permanent molar. Am. J. Phys. Anthropol. 159, 93–105.

Bailey, S.E., Benazzi, S., Hublin, J.-J., 2014. Allometry, merism and tooth shape of the upper second deciduous molar and first permanent molar. Am. J. Phys. Anthropol. 154, 104–114.

Bayle, P., 2008. Proportions des tissus des dents déciduales chez deux individus de Dordogne (France) : l'enfant Néanderthalien du Roc de Marsal et le spécimen du Paléolithique supérieur final de La Madeleine. Bull. Mem. Soc. Anthrop. Paris 20, 151–163.

Bayle, P., Bondioli, L., Macchiarelli, R., Mazurier, A., Puymerail, L., Volpato, V., Zanolli, C., 2011. Three-dimensional imaging and quantitative characterization of human fossil remains. Examples from the NESPOS database. In: Macchiarelli, R., Weniger, G.-C. (Eds.), Pleistocene Databases. Acquisition, Storing, Sharing. Wissenschaftliche Schriften des Neanderthal Museums 4, Mettmann, pp. 29–46.

Bayle, P., Braga, J., Mazurier, A., Macchiarelli, R., 2009. Dental developmental pattern of the Neanderthal child from Roc de Marsal: a high-resolution 3D analysis. J. Hum. Evol. 56, 66–75.

Benazzi, S., Fornai, C., Bayle, P., Coquerelle, M., Kullmer, O., Mallegni, F., Weber, G.W., 2011. Comparison of dental measurement systems for taxonomic assignment of Neanderthal and modern human lower second deciduous molars. J. Hum. Evol. 61, 320–326.

Benazzi, S., Nguyen, H.N., Kullmer, O., Hublin, J.-J., 2013a. Unravelling the functional biomechanics of dental features and tooth wear. PLoS One 8, e69990, http://dx.doi.org/10.1371/journal.pone.0069990.

Benazzi, S., Nguyen, H.N., Schulz, D., Grosse, I.R., Gruppioni, G., Hublin, J.-J., Kullmer, O., 2013b. The evolutionary paradox of tooth wear: simply destruction or inevitable adaptation? PLoS One 8, e62263, http://dx.doi.org/10.1371/journal.pone.0062263.

Bondioli, L., Bayle, P., Dean, C., Mazurier, A., Puymerail, L., Ruff, C., Stock, J.T., Volpato, V., Zanolli, C., Macchiarelli, R., 2010. Morphometric maps of long bone shafts and dental roots for imaging topographic thickness variation. Am. J. Phys. Anthropol. 142, 328–334.

Butler, P.M., 1956. The ontogeny of molar pattern. Biol. Rev. 31, 30–69.

Butler, P.M., 1967. Comparison of the development of the second deciduous molar and first permanent molar in man. Arch. Oral Biol. 12, 1245–1260.

Chan, E., Bockmann, M., Hughes, T., Mihailidis, S., Townsend, G., 2012. Do feeding practices, gestation length, and birth weight affect the timing of emergence of the first primary tooth? In: Townsend, G., Kanazawa, E., Takayama, H. (Eds.), New Directions in Dental Anthropology. The University of Adelaide Press, Adelaide, pp. 35–45.

Coleman, M.N., Colbert, M.W., 2007. Technical note: CT thresholding protocols for taking measurements on three-dimensional models. Am. J. Phys. Anthropol. 133, 723–725.

Constantino, P.J., Lee, J.J.W., Gerbig, Y., Hartstone-Rose, A., Talebi, M., Lawn, B.R., Lucas, P.W., 2012. The role of tooth enamel mechanical properties in primate dietary adaptation. Am. J. Phys. Anthropol. 148, 171–177.

Constantino, P.J., Lee, J.J.W., Morris, D., Lucas, P.W., Hartstone-Rose, A., Lee, W.K., Dominy, N.J., Cunningham, A., Wagner, M., Lawn, B.R., 2011. Adaptation to hard object feeding in sea otters and hominins. J. Hum. Evol. 61, 89–96.

Cuozzo, F.P., Ungar, P.S., Sauther, M.L., 2012. Primate dental ecology: how teeth respond to the environment. Am. J. Phys. Anthropol. 148, 159–162.

Daubert, D.M., Kelley, J.L., Udod, Y.G., Habor, C., Kleist, G.C., Furman, I.K., Tikonov, I.N., Swanson, W.J., Roberts, F.A., 2016. Human enamel thickness and ENAM polymorphism. Intl. J. Oral. Sci. 8, 93–97.

Dean, M.C., 2000. Progress in understanding hominoid dental development. J. Anat. 197, 77–101.

Dean, M.C., 2006. Tooth microstructure tracks the pace of human life history evolution. Proc. Roy. Soc. B 273, 2799–2808.

Dean, M.C., 2010. Retrieving chronological age from dental remains of early fossil hominins to reconstruct human growth in the past. Phil. Trans. Roy. Soc. B 365, 3397–3410.

Dean, M.C., Cole, T.J., 2013. Human life history evolution explains dissociation between the timing of tooth eruption and peak rates of root growth. PLoS One 8, e54534, http://dx.doi.org/10.1371/journal.pone.0054534.

Dean, M.C., Jones, M.E., Pilley, J.R., 1992. The natural history of tooth wear, continuous eruption and periodontal disease in wild shot great apes. J. Hum. Evol. 22, 23–39.

Dowdeswell, M.R., Jashashvili, T., Patel, B.A., Lebrun, R., Susman, R.L., Lordkipanidze, D., Carlson, K.J., 2017. Adaptation to bipedal gait and fifth metatarsal structural properties in *Australopithecus*, Paranthropus, and Homo. C. R. Palevol, https://doi.org/10.1016/j.crpv.2016.10.003.

Evans, A.R., Daly, E.S., Catlett, K.K., Paul, K.S., King, S.J., Skinner, M.M., Nesse, H.P., Hublin, J.-J., Townsend, G.C., Schwartz, G.T., Jernvall, J., 2016. A simple rule governs the evolution and development of hominin tooth size. Nature 530, 477–480.

Fajardo, R.J., Ryan, T.M., Kappelman, J., 2002. Assessing the accuracy of high-resolution X-ray computed tomography of primate trabecular bone by comparisons with histological sections. Am. J. Phys. Anthropol. 118, 1–10.

Feeney, R.N.M., Zermeno, J.P., Reid, D.J., Nakashima, S., Sano, H., Bahar, A., Hublin, J.-J., Smith, T.M., 2010. Enamel thickness in Asian human canines and premolars. Anthropol. Sc. 118, 191–198.

Fleagle, J.G., 2013. Primate Adaptation and Evolution, third ed. Elsevier, London.

Fornai, C., Benazzi, S., Gopher, A., Barkai, R., Sarig, R., Bookstein, F.L., Hershkovitz, I., Weber, G.W., 2016. The Qesem Cave hominin material

(part 2): a morphometric analysis of dm2-QC2 deciduous lower second molar. Quatern. Int. 398, 175–189.
Fornai, C., Benazzi, S., Svoboda, J., Pap, I., Harvati, K., Weber, G., 2014. Enamel thickness variation of deciduous first and second upper molars in modern humans and Neanderthals. J. Hum. Evol. 76, 83–91.
Gantt, D.G., Harris, E.F., Rafter, J.A., Rahn, J.K., 2001. Distribution of enamel thickness on human deciduous molars. In: Brook, A. (Ed.), Dental Morphology 2001. Sheffield Academic Press, Sheffield, pp. 167–190.
Grine, F.E., 2005. Enamel thickness of deciduous and permanent molars in modern *Homo sapiens*. Am. J. Phys. Anthropol. 126, 14–31.
Grine, F.E., Daegling, D.J., 2017. Functional morphology, biomechanics and the retrodiction of early hominin diets. C. R. Palevol, https://doi.org/10.1016/j.crpv.2017.01.005.
Grine, F.E., Martin, L.B., 1988. Enamel thickness and development in *Australopithecus* and *Paranthropus*. In: Grine, F.E. (Ed.), Evolutionary History of the "Robust" Australopithecines. Aldine de Gruyter, New York, pp. 3–42.
Guatelli-Steinberg, D., 2016. What Teeth Reveal about Human Evolution. Cambridge University Press, Cambridge.
Guy, F., Gouvard, F., Boistel, R., Euriat, A., Lazzari, V., 2013. Prospective in (Primate) dental analysis through tooth 3D topographical quantification. PLoS One 8, e66142, http://dx.doi.org/10.1371/journal.pone.0066142.
Hartwig, W.C., 2002. The Primate Fossil Record. Cambridge University Press, Cambridge.
Hemmer, H., 2015. Estimation of basic life history data of fossil hominoids. In: Henke, W., Tattersall, I. (Eds.), Handbook of Paleoanthropology. Springer-Verlag, Berlin, pp. 703–743.
Hlusko, L.J., 2016. Elucidating the evolution of hominid dentition in the age of phenomics, modularity, and quantitative genetics. Ann. Anat. 203, 3–11.
Hlusko, L.J., Suwa, G., Kono, R.T., Mahaney, C., 2004. Genetics and the evolution of primate enamel thickness: a baboon model. Am. J. Phys. Anthropol. 124, 223–233.
Horvath, J.E., Ramachandran, G.L., Fedrigo, O., Nielsen, W.J., Babbitt, C.C., St. Clair, E.M., Pfefferle, L.W., Jernvall, J., Wray, G.A., Wall, C.E., 2014. Genetic comparisons yield insight into the evolution of enamel thickness during human evolution. J. Hum. Evol. 73, 75–87.
Huszár, G., 1972. Enamel thickness of deciduous teeth. Fogorvosi Szemle 65, 133–137 (original in Hungarian).
Kato, A., Tang, N., Borries, C., Papakyrikos, A.M., Hinde, K., Miller, E., Kunimatsu, Y., Hirasaki, E., Shimizu, D., Smith, T.M., 2014. Intra- and interspecific variation in macaque molar enamel thickness. Am. J. Phys. Anthropol. 155, 447–459.
Kelley, J., Bolter, D., 2013. Growth, development, and life history in hominin evolution. In: Begun, D.R. (Ed.), A Companion to Paleoanthropology. John Wiley & Sons, Chichester, pp. 97–117.
Kelley, J.L., Swanson, W.J., 2008. Dietary change and adaptive evolution of enamelin in humans and among primates. Genetics 178, 1595–1603.
Kono, R., 2004. Molar enamel thickness and distribution patterns in extant great apes and humans: new insights based on a 3-dimensional whole crown perspective. Anthropol. Sci. 112, 121–146.
Kono, R., Suwa, G., 2008. Enamel distribution patterns of extant human and hominoid molars: occlusal versus lateral enamel thickness. Bull. Natl. Mus. Nat. Sci. Ser. D 34, 1–9.
Kono, R.T., Suwa, G., Tanijiri, T., 2002. A three-dimensional analysis of enamel distribution patterns in human permanent first molars. Arch. Oral Biol. 47, 867–875.
Kono, R.T., Zhang, Y., Jin, C., Takai, M., Suwa, G., 2014. A 3-dimensional assessment of molar enamel thickness and distribution pattern in *Gigantopithecus blacki*. Quat. Int. 354, 46–51.
Kraus, B., Jordan, R., 1965. The Human Dentition Before Birth. Lea and Febiger, Philadelphia.
Le Luyer, M., (PhD dissertation) 2016. Évolution dentaire dans les populations humaines de la fin du Pléistocène et du début de l'Holocène (19 000–5500 cal. BP) : une approche intégrée des structures externe et interne des couronnes pour le Bassin Aquitain et ses marges. Université de Bordeaux, Bordeaux.
Le Luyer, M., Bayle, P., 2017. Outer and inner structural variation of upper molars in Late Pleistocene and Early Holocene humans: morphological and functional interpretations. C. R. Palevol, http://dx.doi.org/10.1016/j.crpv.2016.11.009.
Lucas, P., Constantino, P., Wood, B., Lawn, B.R., 2008. Dental enamel as a dietary indicator in mammals. Bioessays 30, 374–385.
Macchiarelli, R., Bayle, P., Bondioli, L., Mazurier, A., Zanolli, C., 2013. From outer to inner structural morphology in dental anthropology. The integration of the third dimension in the visualization and quantitative analysis of fossil remains. In: Scott, R.G., Irish, J.D. (Eds.), Anthropological Perspectives on Tooth Morphology: Genetics, Evolution, Variation. Cambridge University Press, Cambridge, pp. 250–277.
Macchiarelli, R., Bayle, P., Zanolli, C., Braga, J., 2016. Why in 3-4D? What new insights virtual imaging are revealing in dental (palaeo)anthropology. Am. J. Phys. Anthropol. 159 (S62), 214 (abstract).
Macchiarelli, R., Bondioli, L., Debénath, A., Mazurier, A., Tournepiche, J.F., Birch, W., Dean, C., 2006. How Neanderthal molar teeth grew. Nature 444, 748–751.
Macchiarelli, R., Bondioli, L., Falk, D., Faupl, P., Illerhaus, B., Kullmer, O., Richter, W., Said, H., Sandrock, O., Schäfer, K., Urbanek, C., Viola, B.T., Weber, G.W., Seidler, H., 2004. Early Pliocene hominid tooth from Galili, Somali Region, Ethiopia. Coll. Antropol. 28, 65–76.
Macchiarelli, R., Bondioli, L., Mazurier, A., 2008. Virtual dentitions: touching the hidden evidence. In: Irish, J.D., Nelson, G.C. (Eds.), Technique and Application in Dental Anthropology. Cambridge University Press, Cambridge, pp. 426–448.
Macchiarelli, R., Mazurier, A., Illerhaus, B., Zanolli, C., 2009. *Ouranopithecus macedoniensis* (Mammalia, Primates, Hominoidea): virtual reconstruction and 3D analysis of a juvenile mandibular dentition (RPl-82 and RPl-83). Geodiver. 31, 851–864.
Macho, G.A., 2015. General principles of evolutionary morphology. In: Henke, W., Tattersall, I. (Eds.), Handbook of Paleoanthropology. Springer-Verlag, Berlin, pp. 921–936.
Macho, G.A., Berner, M.E., 1993. Enamel thickness of human maxillary molars reconsidered. Am. J. Phys. Anthropol. 92, 189–200.
Mahoney, P., 2010. Two-dimensional patterns of human enamel thickness on deciduous (dm1, dm2) and permanent first (M1) mandibular molars. Arch. Oral Biol. 55, 115–126.
Mahoney, P., 2013. Testing functional and morphological interpretations of enamel thickness along the deciduous tooth row in human children. Am. J. Phys. Anthropol. 151, 518–525.
Martin, L.B., 1985. Significance of enamel thickness in hominoid evolution. Nature 314, 260–263.
Martin, L.B., Olejniczak, A.J., Maas, M.C., 2003. Enamel thickness and microstructure in pitheciin primates, with comments on dietary adaptations of the middle Miocene hominoid *Kenyapithecus*. J. Hum. Evol. 45, 351–367.
Merceron, G., Blondel, C., de Bonis, L., Koufos, G.D., Viriot, L., 2005. A new method of dental microwear analysis: application to extant primates and *Ouranopithecus macedoniensis* (Late Miocene of Greece). Palaios 20, 551–561.
Mitteroecker, P., Bookstein, F.L., 2011. Linear discrimination, ordination, and the visualization of selection gradients in modern morphometrics. Evol. Biol. 38, 100–114.
Morita, W., Morimoto, N., Kunimatsu, Y., Mazurier, A., Zanolli, C., Nakatsukasa, M., 2017. A morphometric mapping analysis of lower fourth deciduous premolar in hominoids: implications for phylogenetic relationship between *Nakalipithecus* and *Ouranopithecus*. C. R. Palevol, https://doi.org/10.1016/j.crpv.2016.10.004.
Morita, W., Morimoto, N., Ohshima, H., 2016. Exploring metameric variation in human molars: a morphological study using morphometric mapping. J. Anat. 229, 343–355.
Nelson, S.V., Rook, L., 2016. Isotopic reconstructions of habitat change surrounding the extinction of *Oreopithecus*, the last European ape. Am. J. Phys. Anthropol. 160, 254–271.
NESPOS Database, 2017. Neanderthal Studies Professional Online Service. http://www.nespos.org.
Olejniczak, A.J., Smith, T.M., Feeney, R.N.M., Macchiarelli, R., Mazurier, A., Bondioli, L., Rosas, A., Fortea, J., de la Rasilla, M., García-Tabernero, A., Radovčić, J., Skinner, M.M., Toussaint, M., Hublin, J.-J., 2008a. Dental tissue proportions and enamel thickness in Neandertal and modern human molars. J. Hum. Evol. 55, 12–23.
Olejniczak, A.J., Smith, T.M., Skinner, M.M., Grine, F.E., Feeney, R.N.M., Thackeray, F.J., Hublin, J.-J., 2008b. Three-dimensional molar enamel distribution and thickness in *Australopithecus* and *Paranthropus*. Biol. Lett. 4, 406–410.
Olejniczak, A.J., Smith, T.M., Wang, W., Potts, R., Ciochon, R., Kullmer, O., Schrenk, F., Hublin, J.-J., 2008c. Molar enamel thickness and dentine horn height in *Gigantopithecus blacki*. Am. J. Phys. Anthropol. 135, 85–91.
Olejniczak, A.J., Tafforeau, P., Feeney, R.N.M., Martin, L.B., 2008d. Three-dimensional primate molar enamel thickness. J. Hum. Evol. 54, 187–195.
Pampush, J.D., Duque, A.C., Burrows, B.R., Daegling, D.J., Kenney, W.F., McGraw, W.S., 2013. Homoplasy and thick enamel in primates. J. Hum. Evol. 64, 216–224.
Pan, L., Dumoncel, J., de Beer, F., Hoffman, J., Thackeray, J.F., Duployer, B., Tenailleau, C., Braga, J., 2016. Further morphological evidence

on South African earliest *Homo* lower postcanine dentition: enamel thickness and enamel-dentine junction. J. Hum. Evol. 96, 82–96.
Pebesma, E.J., 2004. Multivariable geostatistics in S: the gstat package. Comp. Geosc. 30, 683–691.
Peretto, C., Arnaud, J., Moggi-Cecchi, J., Manzi, G., Nomade, S., Pereira, A., Arzarello, M., 2015. A human deciduous tooth and new $^{40}Ar/^{39}Ar$ dating results from the Middle Pleistocene archaeological site of Isernia La Pineta, southern Italy. PLoS One 10, e0140091, http://dx.doi.org/10.1371/journal.pone.0140091.
Puymerail, L., (Ph.D. dissertation) 2011. Caractérisation de l'endostructure et des propriétés biomécaniques de la diaphyse fémorale : la signature de la bipédie et la reconstruction des paléo-répertoires posturaux et locomoteurs des Hominiés. Muséum national d'histoire naturelle, Paris.
Puymerail, L., Ruff, C.B., Bondioli, L., Widianto, H., Trinkaus, E., Macchiarelli, R., 2012a. Structural analysis of the Kresna 11 *Homo erectus* femoral shaft (Sangiran, Java). J. Hum. Evol. 63, 741–749.
Puymerail, L., Volpato, V., Debénath, A., Mazurier, A., Tournepiche, J.F., Macchiarelli, R., 2012b. A Neanderthal partial femoral diaphysis from the "grotte de la Tour", La Chaise-de-Vouthon (Charente, France): outer morphology and endostructural organization. C. R. Palevol 11, 581–593.
R Development Core Team, 2017. R: A Language and Environment for Statistical Computing. http://www.r-project.org.
Rabenold, D., Pearson, O.M., 2011. Abrasive, silica phytoliths and the evolution of thick molar enamel in primates, with implications for the diet of *Paranthropus boisei*. PLoS One 6, e28379, http://dx.doi.org/10.1371/journal.pone.0028379.
Rossi, P.F., Bondioli, L., Geusa, G., Macchiarelli, R., 1999. Osteodental biology of the people of *Portus Romae* (necropolis of Isola Sacra, 2nd–3rd cent. AD). I. Enamel microstructure and developmental defects of the primary dentition. In: Bondioli, L., Macchiarelli, R. (Eds.), Digital Archives of Human Paleobiology, 1. E-LISA, Milano (CD-ROM).
Schlager, S., 2017. Morpho: Calculations and Visualisations Related to Geometric Morphometrics. https://CRAN.R-project.org/package=Morpho.
Schneider, C.A., Rasband, W.S., Eliceiri, K.W., 2012. NIH Image to ImageJ: 25 years of image analysis. Nat. Methods 9, 671–675.
Schwartz, G.T., 2000b. Enamel thickness and the helicoidal wear plane in modern human mandibular molars. Arch. Oral Biol. 45, 401–409.
Schwartz, G.T., 2000a. Taxonomic and functional aspects of the patterning of enamel thickness distribution in extant large-bodied hominoids. Am. J. Phys. Anthropol. 111, 221–244.
Scott, R.S., Ungar, P.S., Bergstrom, T.S., Brown, C.A., Grine, F.E., Teaford, M.T., Walker, A., 2005. Dental microwear texture analysis shows within-species diet variability in fossil hominins. Nature 436, 693–695.
Simmer, J.P., Papagerakis, P., Smith, C.E., Fisher, D.C., Rountrey, A.N., Zheng, L., Hu, J.C.C., 2010. Regulation of dental enamel shape and hardness. J. Dent. Res. 89, 1024–1038.
Skinner, M.M., Alemseged, Z., Gaunitz, C., Hublin, J.-J., 2015. Enamel thickness trends in Plio-Pleistocene hominin mandibular molars. J. Hum. Evol. 85, 35–45.
Smith, T.M., Bacon, A.-M., Demeter, F., Kullmer, O., Nguyen, K.T., de Vos, J., Wei, W., Zermeno, J.P., Zhao, L., 2011. Dental tissue proportions in fossil orangutans from mainland Asia and Indonesia. Hum. Origins Res. 1, e1, http://dx.doi.org/10.4081/hor.2011.e1.
Smith, T.M., Martin, L.B., Leakey, M.G., 2003. Enamel thickness, microstructure and development in *Afropithecus turkanensis*. J. Hum. Evol. 44, 283–306.
Smith, T.M., Olejniczak, A.J., Martin, L.B., Reid, D.J., 2005. Variation in hominoid molar enamel thickness. J. Hum. Evol. 48, 575–592.
Smith, T.M., Olejniczak, A.J., Zermeno, J.P., Tafforeau, P., Skinner, M.M., Hoffmann, A., Radovčić, J., Toussaint, M., Kruszynski, R., Menter, C., Moggi-Cecchi, J., Glasmacher, U.A., Kullmer, O., Schrenk, F., Stringer, C., Hublin, J.-J., 2012. Variation in enamel thickness within the genus *Homo*. J. Hum. Evol. 62, 395–411.
Sponheimer, M., Lee-Thorp, J., 2015. Hominin paleodiets: the contribution of stable isotopes. In: Henke, W., Tattersall, I. (Eds.), Handbook of Paleoanthropology. Springer-Verlag, Berlin, pp. 671–701.
Spoor, F., Zonneveld, F., Macho, G.A., 1993. Linear measurements of cortical bone and dental enamel by computed tomography: applications and problems. Am. J. Phys. Anthropol. 91, 469–484.
Suwa, G., Kono, R.T., Simpson, S.W., Asfaw, B., Lovejoy, C.O., White, T.D., 2009. Paleobiological implications of the *Ardipithecus ramidus* dentition. Science 326, 94–99.
Swindler, D.R., 2002. The Primate Dentition. An Introduction to the Teeth of Non-Human Primates. Cambridge University Press, Cambridge.
Teaford, M.F., 2007. What do we know and not know about diet and enamel structure? In: Ungar, P.S. (Ed.), Evolution of the Human Diet: The Known, the Unknown, and the Unknowable. Oxford University Press, New York, pp. 56–76.
Teaford, M.F., Ungar, P.S., 2015. Dental adaptations of African apes. In: Henke, W., Tattersall, I. (Eds.), Handbook of Paleoanthropology. Springer-Verlag, Berlin, pp. 1465–1493.
Toussaint, M., Olejniczak, A.J., El Zaatari, S., Cattelain, P., Flas, D., Letourneux, C., Pirson, S., 2010. The Neandertal lower right deciduous second molar from Trou de l'Abîme at Couvin, Belgium. J. Hum. Evol. 58, 56–67.
Tsegai, Z.J., Stephens, N.B., Treece, G.M., Skinner, M.M., Kivell, T.L., Geeba, A.H., 2017. Cortical bone mapping: an application to hand and foot bones in hominoids. C. R. Palevol, https://doi.org/10.1016/j.crpv.2016.11.001.
Ungar, P.S. (Ed.), 2007. Evolution of the Human Diet: The Known, the Unknown, and the Unknowable. Oxford University Press, New York.
Ungar, P.S., Sponheimer, M., 2013. Hominin diets. In: Begun, D.R. (Ed.), A Companion to Paleoanthropology. John Wiley & Sons, Chichester, pp. 165–182.
Vogel, E.R., van Woerden, J.T., Lucas, P.W., Atmoko, S.S.U., van Schaik, C.P., Dominy, N.J., 2008. Functional ecology and evolution of hominoid molar enamel thickness: *Pan troglodytes schweinfurthii* and *Pongo pygmaeus wurmbii*. J. Hum. Evol. 55, 60–74.
Zanolli, C., 2015a. Molar crown inner structural organization in Javanese *Homo erectus*. Am. J. Phys. Anthropol. 156, 148–157.
Zanolli, C., 2015b. L'épaisseur de l'émail comme indicateur adaptatif écosensible. Comment varie-t-elle entre dents déciduales et permanentes chez les hominidés actuels et fossiles ? Bull. Mem. Soc. Anthropol. Paris 27, S28–S29 (abstract).
Zanolli, C., Bayle, P., Macchiarelli, R., 2010a. Tissue proportions and enamel thickness distribution in the early Middle Pleistocene human deciduous molars from Tighenif (Ternifine), Algeria. C. R. Palevol 9, 341–348.
Zanolli, C., Bondioli, L., Coppa, A., Dean, M.C., Bayle, P., Candilio, F., Capuani, S., Dreossi, D., Fiore, I., Frayer, D.W., Libsekal, Y., Mancini, L., Rook, L., Medin Tekle, T., Tuniz, C., Macchiarelli, R., 2014. The late Early Pleistocene human dental remains from Uadi Aalad and Mulhuli-Amo (Buia), Eritrean Danakil: Macromorphology and microstructure. J. Hum. Evol. 74, 96–113.
Zanolli, C., Bondioli, L., Mancini, L., Mazurier, A., Widianto, H., Macchiarelli, R., 2012. Two human fossil deciduous molars from the Sangiran Dome (Java, Indonesia): outer and inner morphology. Am. J. Phys. Anthropol. 147, 472–481.
Zanolli, C., Cantaloube, M., Bayle, P., Bondioli, L., Dumoncel, J., Durrleman, S., Jessel, J.P., Subsol, G., Macchiarelli, R., 2016b. Innovative approaches to quantify and statistically compare tooth enamel thickness distribution. Proc. Europ. Soc. Hum. Evol. 5, 251 (abstract).
Zanolli, C., Dean, M.C., Rook, L., Bondioli, L., Mazurier, A., Macchiarelli, R., 2016a. Enamel thickness and enamel growth in *Oreopithecus*: combining microtomographic and histological evidence. C. R. Palevol 15, 209–226.
Zanolli, C., Grine, F.E., Kullmer, O., Schrenk, F., Macchiarelli, R., 2015. Brief Communication: The Early Pleistocene deciduous hominid molar FS-72 from the Sangiran Dome of Java, Indonesia: a taxonomic reappraisal based on its comparative endostructural characterization. Am. J. Phys. Anthropol. 157, 666–674.
Zanolli, C., Le Luyer, M., Balaresque, P., Bayle, P., Esclassan, R., Maret, D., Vaysse, F., 2017. Exploration de la variabilité de la structure des tissus dentaires dans les populations humaines (sub)actuelles. Bull. Mem. Soc. Anthropol. Paris 29, S33 (abstract).
Zanolli, C., Rook, L., Macchiarelli, R., 2010b. Analyse structurale à haute résolution des dents de *Oreopithecus bambolii*. Ann. Univ. Ferrara Mus. Sci. Nat. 6, 69–76.